

Turning Cold Tumors Hot: Exploring Whether Val-boroPro
and Val-boroPro and Doxorubicin Exhibit Synergy in the
CT-26 Mouse Tumor Model

A thesis submitted by

Victoria Margosian

in partial fulfillment of the requirements for the degree of

Master of Science

in

Pharmacology and Drug Development

Tufts University

Sackler School of Graduate Biomedical Sciences

August 2019

Advisor: William W. Bachovchin, Ph.D

Abstract

Val-boroPro, a compound first synthesized in the Bachovchin Lab at Tufts University Sackler School of Graduate Biomedical Sciences as a dipeptidyl aminopeptidase inhibitor, was found to stimulate the production of specific cytokines that enhance the immune response to tumors in a variety of mouse models. However, in these models, a criteria observed to mediate Val-boroPro's efficacy was the immunogenicity of the cancer cell line targeted for treatment. In non-antigenically visible cancers, Val-boroPro failed to elicit the same level of anti-cancer activity, as with those cancers that were known to be antigenically visible to the hosts immune system. This is feature that is common across immuno-oncology agents, as only immunogenic cancers elicit the recruitment of both the innate and the adaptive immune system. In contrast, those cancers that are not antigenically visible only recruit an innate immune response, which dramatically reduces their anti-cancer activity.

Doxorubicin is an approved chemotherapeutic agent that interferes with DNA repair mechanisms, and causes cell death by necroptosis. Recent literature suggests that Doxorubicin is one of several chemotherapeutic agents that is able to induce immunogenic cell death of tumor cells. This inference followed the observation that Doxorubicin has greater anti-cancer activity in immune competent animals than in xenograft models. It is speculated that such a form of cell death might make the tumor antigenically visible to the hosts immune system.

My masters' thesis hypothesizes that Val-boroPro will synergize with compounds such as doxorubicin that induce immunogenic cell death. To test this hypothesis, a combination of Val-boroPro and Doxorubicin were administered to Balb/c mice

inoculated with syngeneic tumor model CT-26, which is a model for colon cancer, and for which Doxorubicin induced immunogenic cell death has been previously observed. The objective of my project was to determine if Val-boroPro immune enhancing activity could be harnessed in non-antigenically visible cancers when it was given with Doxorubicin.

Acknowledgements

I would like to thank Tufts University and the Sackler School of Graduate Biomedical Sciences for the resources and learning opportunities it provided me, which afforded me the opportunity and to complete this thesis. I would also like to thank Bachovchin lab team members, Christina Deliyiannis, Barry Jones, Jack Lai, Sarah Poplawski, David Sanford, and Yuhong Zhou, who collectively assisted me with obtaining the training required for the successful execution of this research project. I would also like to thank all of my Pharmacology and Drug Development peers, both in my cohort and those in the years above and below me, for their unwavering support and encouragement of me throughout my time at Tufts. Finally, I'd like to issue a very special statement of gratitude to Dr. William Bachovchin. Your generosity in accepting me into your lab and spending the time required to guide me towards my interests has defined my experience at Tufts and has enabled my future direction. Without your dedication, encouragement, time commitment, expertise, patience, and belief in my abilities, the completion of this thesis would not have been possible.

Table of Contents

Title page	i
Abstract	ii
Acknowledgements.....	iv
Table of Contents	v
List of Tables	vii
List of Figures.....	viii
List of Abbreviations	ix
Chapter 1. Introduction	1
1.1 History of Immunotherapy in Oncology.....	1
1.2 Immunotherapeutic Challenges & Requirements	2
1.3 Val-boroPro in the Context of Immunotherapeutic Challenges	3
1.4 Challenges Val-boroPro Monotherapy Fails to Address	3
1.5 CT-26 Tumor Cell Line in the Context of Immunotherapy.....	6
1.6 Xaa-boroPro's and the discovery of the DASH Family	8
1.7 DASH Substrate Specificity	10
1.8 Val-boroPro's Anticancer Mechanism of Action	11
1.9 Expanded mechanistic Understanding of Val-boroPro Anticancer Mechanism.....	14
1.10 Val-boroPro's Clinical History.....	16
1.11 Elucidating the Mechanism of Val-boroPro Toxicities	17
1.12 Experimental Rationale & Doxorubicin as an Immunogenic Chemotherapeutic Agent	18
1.13 Chapter 1 notes	19
Chapter 2. Materials and Methods	20
2.1 Animals.....	20
2.2 Tumor Cell Line and <i>in vitro</i> Culture	20
2.3 Therapeutic Agents and Formulation.....	20
2.4 Tumor Inoculation and Protocol	22
2.4.1 Group Assignments.....	23
2.4.2 Tumor Measurements	24
2.4.3 Drug Doses and Schedule of Administration.....	26
2.5 Statistical Analysis.....	27
2.6 Chapter 2 notes	27
Chapter 3. Results	28
3.1 Tumor Size.....	28

3.2	Body weights	32
3.3	Survival Time.....	33
3.4	Chapter 3 notes	34
Chapter 4. Discussion		35
Chapter 5. Bibliography.....		37

List of Tables

Table 1.1. Xaa-boroPro IC50 Values for DASH Family Members	12
Table 1.2. Val-boroPro Clinical Indication.....	16
Table 1.3. Val-boroPro Phase 2 and 3 Clinical Programs.....	17
Table 2.1 Mouse Groupings Mean Weight and Tumor Volume.....	23
Table 2.2 Individual Mouse Tumor Volumes at the Time of Grouping.....	24
Table 2.3. Tumor Measurement Schedule	25
Table 2.4. Group Treatment Schedules	26
Table 2.5. Inoculation and Dosing Schedule.....	27
Table 3.1 Tumor Volumes by Mouse	30
Table 3.2 Mouse Body Weights	33

List of Figures

Figure 1.1. Immunogenic Verse Non-Immunogenic Cancer Following Treatment with Xaa-boroPro.....	5
Figure 1.2. Val-boroPro Efficacy in CT-26 Mice	7
Figure 1.3. DASH Family Overview	9
Figure 1.4. DASH Family Specificity.....	10
Figure 1.5. Val-boroPro T-cell Dependence	15
Figure 2.1 Val-boroPro.....	21
Figure 2.2 Doxorubicin	22
Figure 3.1. Aggregated Tumor Volumes by Treatment	28
Figure 3.2 Mouse Tumor Volumes Broken Out by Group.....	29
Figure 3.3. Statistical Comparison of Tumor Volume	31
Figure 3.4 Mouse Body Weights by Group.....	32
Figure 3.5 Survival Curve	34

List of Abbreviations

CD20: cluster of differentiation 20
CD33: cluster of differentiation 33
CD50: cluster of differentiation 50
CARs: chimeric antigen receptors
CTLA4: cytotoxic T-lymphocyte-associated protein 4
DASH; DPPIV structure and activity homologs
DLAM: department of laboratory animal management
DPP2; dipeptidyl peptidase 2
DPP6; dipeptidyl peptidase 6
DPP8; dipeptidyl peptidase 8
DPP9; dipeptidyl peptidase 9
DPPIV; dipeptidyl peptidase 4
ECM; extracellular matrix
EGFR: human epidermal growth factor receptor 2
FAP; fibroblast activation protein
FBS: fetal bovine serum
Her2: human epidermal growth factor receptor 2
IACUC: Institutional Animal Care and Use Committee
IL-1 β ; interleukin 1 β
IL-2: interleukin 2
IL-6; interleukin 6
IO: immune-oncology
KO; knockout
NSCLC; non-small cell lung cancer
PDL-1: programmed death receptor ligand 1
PREP; prolyl oligopeptidase
USAN: united states adopted name
Xaa-boroPro; dipeptide boro-proline

Chapter 1. Introduction

Immuno-oncology seeks to enhance the body's existing, but generally ineffective immune response to tumors [1]. Most often, IO agents do not seek to generate a new immune response, but instead, these agents work to optimize existing immune activity, which has already been mounted by the host against the tumor [1].

In non-antigenically visible tumors, an anti-cancer immune response is carried out by cells of the innate immune [1]. This innate immune response generally stalls the cancer for some period of time while the cancer is in its initial stages [2]. However, it does not provide significant benefit in containing cancer that is metastatic [1].

In antigenically visible tumors, a second immune response is present, which proceeds through the adaptive immune system [1]. Antigenically visible cancers benefit significantly from their generation of both an innate and an adaptive immune response [1]. Similar, IO agents benefit from cancers that generate a dual response to tumors, as this affords these agents access to two pathways to optimize, and these agents are almost ubiquitously more effective at treating cancers that generate antigenic stimulus than at treating cancers that do not have an antigenic component [1].

1.1 History of Immunotherapy in Oncology

Cancer has long been speculated to be a disease of the immune system, in which carcinogenic cells are permitted to survive and proliferate in the absence of an effective immune response [1]. The role of the immune system in containing carcinomas was substantiated with the proof-of-concept clinical trial utilizing anti-CTLA4 [1]. CTLA4 is a protein receptor that functions as an immune checkpoint and works by downregulating

the response of cytotoxic T-cells. Anti-CTLA4 therapy inhibits this checkpoint and blocks the associated downregulation in cytotoxic T-cell function.

Since the validation of CTLA4 as a clinical target, immunotherapies have seen a cascade of approvals for a variety of cancer types and targets. These include the approval of nine different monoclonal antibodies, which target six cancer associated proteins, including Her2, NEU, EGFR, VEGF, CD20, CD52, and CD33 [1]. Additionally, allogeneic bone marrow transplant, which results in the recipient receiving allogeneic donor lymphocytes, has been shown to be a highly effective method of treatment for various forms of leukemia [1]. Other immunotherapies that have demonstrated efficacy and received approval for oncologic targets include, CAR-t which is approved for the treatment of certain types of lymphoma and acute lymphoblastic leukemia, the recombinant cytokine IL-2 which is approved for the treatment of metastatic renal cell carcinoma and metastatic melanoma, and anti-PDL-1 which is approved for metastatic non-small cell lung cancer and head and neck squamous cell carcinoma [1].

1.2 Immunotherapeutic Challenges & Requirements

For immunotherapy to be effective, the following critical immune functions must be carried out. The first of these functions, and the origin of the anti-cancer immune response is antigen presentation. Antigen presentation is dependent on the dendritic cells present in the tumor microenvironment up-taking and recognizing tumor associated epitopes as antigenic, and then proceeding to traffic these antigens to neighboring lymphoid organs, in which the dendritic cells must present the antigen to the resident T-cells [1]. Here the second critical step in mounting an anti-cancer immune response is carried out. In these lymphoid tissues, T-cell priming and activation occurs [1]. The final

step required to enact an immune response against the tumor, is the successful infiltration and recognition of tumor cells by the activated T-cells, which must overcome a highly immunosuppressive tumor microenvironment in order to reach and act on their target [1].

1.3 Val-boroPro in the Context of Immunotherapeutic Challenges

Inherent in Mellman's framework of the required immunological functions outlined in figure 1.1, are many potential challenges that immunotherapy must overcome. One of these challenges is the highly immunosuppressive tumor microenvironment, in which antigens must be recognized and processed by dendritic cells, and through which activated T-cells must infiltrate [1].

Val-boroPro addresses the issues of the immunosuppressive tumor microenvironment by enhancing immune activation and infiltration into the tumor stroma [2]. This is demonstrated by the preclinical assay work done with the compound by the private company, Point Therapeutics. Point Therapeutics preclinical assay work with Val-boroPro revealed that across a wide variety of cancer models, Val-boroPro stimulated tumor-specific T-cell immunity and resulted in the recruitment and trafficking of innate effector cells such as neutrophils, macrophages, and natural killer cells into the tumor stroma [21].

1.4 Challenges Val-boroPro Monotherapy Fails to Address

In addition to the obstacle of an immunosuppressive tumor microenvironment, immunotherapy mandates the presence of a detectable antigen in order to catalyze the desired anti-cancer immune cascade [1]. Thus, it is unsurprising that Val-boroPro is much more effective at treating antigenically visible cancers than at treating immunogenically silent cancer models [9,16].

The efficacy of Xaa-boroPro compounds, and their dependence on the immunogenicity of the cancer model to stimulate anti-cancer activity, was discovered during preclinical mouse work done with the MB49 bladder carcinoma mouse cell [9]. The MB49 cancer cell line expresses the HY male minor histocompatibility antigen complex [16]. In female mice bearing HY-expressing MB49 tumors, Val-boroPro was shown to produce tumor regression and rejection in all of the treated mice [9]. A major part of the antitumor effect in this model appears to result from the ability of Val-boroPro to enhance the T cell response against HY antigen epitopes, as the MB49 tumor response was greatly reduced in male tumor-bearing mice, which are naturally tolerant to the HY antigen complex [9].

Further confirmation of this finding came when Balb/c mice were inoculated with the non-syngeneic M3-9-M mouse cancer cell line, which is a model for embryonal rhabdomyosarcoma [8]. Additionally, female Balb/c mice were again inoculated with the HY-expressing MB49 urothelial carcinoma line. Both the M3-9-M and the MB49 inoculated mice were subsequently treated with closely related Val-boroPro analog, tbutyl-Gly-boroPro [17]. Following treatment, a dramatic divergence in tumor remission and rejection was observed when comparing the tbutyl-Gly-boroPro treated mouse cohort against the control cohort of mice, which were administered saline [17]. As depicted in figure 1.1 with data generated by the Bachovchin lab, the mice receiving tbutyl-Gly-boroPro treatment experienced a remarkable rate of tumor resolution, where as those mice treated with saline alone, ubiquitously continued to experience growth and the progression of their carcinomas.

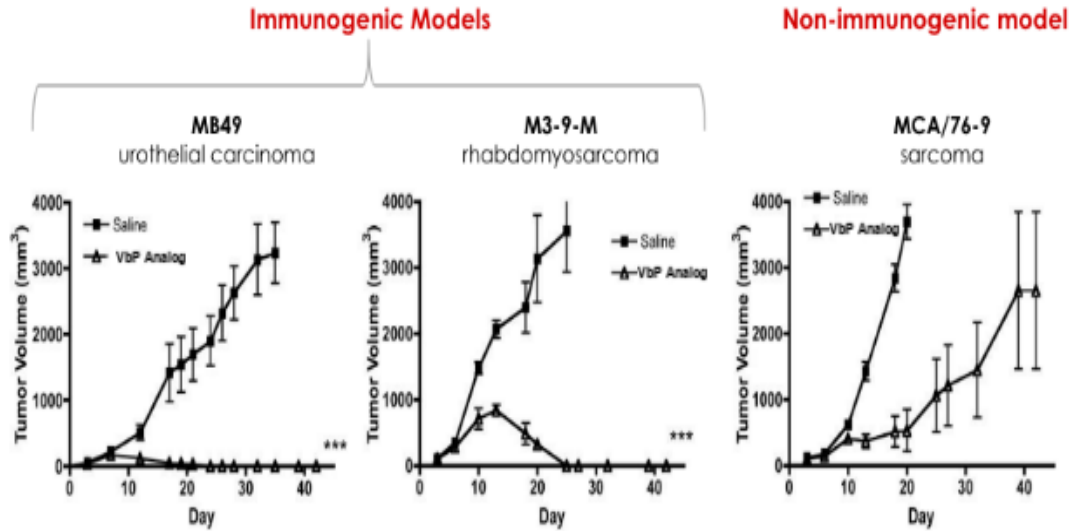


Figure 1.1. Immunogenic Versus Non-Immunogenic Cancer Following Treatment with Xaa-boroPro

Conversely, when Balb/c mouse cohorts were inoculated with the syngeneic mouse cancer cell line MCA/76-9, which models rhabdomyosarcoma and does not express HY-antigens, and those inoculated mice were subsequently treated with tbutyl-Gly-boroPro or saline, treatment resulted in a far less dramatic divergence in efficacy. Data from MCA/76-9 inoculated mice continued to favor tbutyl-Gly-boroPro treatment over saline with respect to stalling the progression in tumor size, but those mice inoculated with MCA/76-9 rhabdomyosarcoma and treated with tbutyl-Gly-boroPro did not experience the tumor regression or rejection observed with non-syngeneic mouse cancer models MB49 and M3-9-M [8, 17].

These results suggest that the antitumor effect of Xaa-boroPro compounds is governed, at least in part, by the intrinsic immunogenicity of the tumor and the strength of the antigenic stimulus it provides to T cells in vivo. It follows that combination therapy with Val-boroPro and an agent that can boost tumor immunogenicity might provide a feasible approach to improving the response of tumors that are refractory to treatment with Val-boroPro by itself.

1.5 CT-26 Tumor Cell Line in the Context of Immunotherapy

CT-26 is a syngeneic mouse cancer cell line that is used as a model for colon cancer. As an antigenically silent cancer, it is unsurprising that Balb/c mice inoculated with the CT-26 cancer cell line and treated with Val-boroPro experienced a similarly stalling in tumor progression and a similar failure to generate tumor regression and rejection, as is seen figure 1.1 with the non-synergic mouse cancer cell line MCA/76-9 treated with tbutyl-Gly-boroPro. This results because in the face of a syngeneic model, antigen cannot be detected by resident dendritic cells in the tumor microenvironment, and therefore an adaptive immune response cannot be generated [1]. Thus, the critical effector cytotoxic T-cells are not activated and primed, and any anti-cancer activity resulting from treatment with Xaa-boroPro compounds in syngeneic models can be solely attributed to the increased response and stimulation of the innate immune system within the tumor microenvironment [1, 21].

Depicted in figure 1.2 with data generated by the Bachovchin lab, is efficacy data regarding Val-boroPro as a treatment to combat Balb/c derived CT-26 mouse colon cancer in Balb/c mice. As is illustrated by these data, as the doses of Val-boroPro administered increases, there is a corresponding delay in tumor progression, however, none of the mice treated with Val-boroPro responded with tumor regression or rejection.

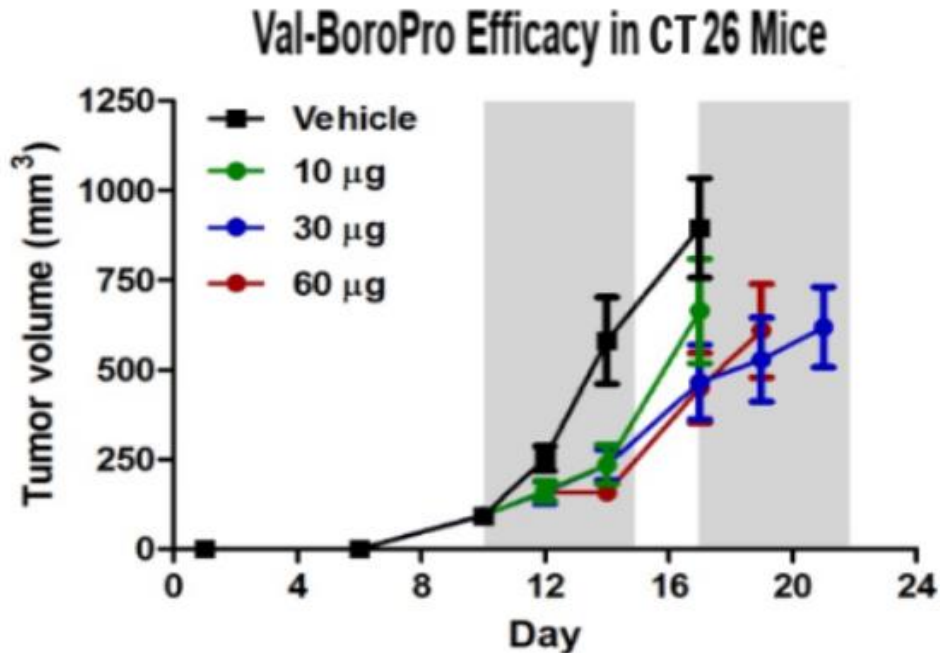


Figure 1.2. Val-boroPro Efficacy in CT-26 Mice

Recent work combining Doxorubicin and immune checkpoint inhibitors, anti-CTLA4 and anti-PD-1, in Balb/c mice inoculated with the syngeneic mouse cancer cell line CT-26, demonstrated a remarkable increase in anti-cancer response rates, when compared to those CT-26 inoculated mice receiving an immune checkpoint inhibitor alone [22]. Of those mice treated with anti-PD-1 monotherapy, 0 out of 10 of the treated mice achieved the complete resolution of their tumor [22]. However, of those mice treated with anti-PD-1 and Doxorubicin combination therapy, 8 of the 10 mice completely recovered from their CT-26 tumor burden [22]. Similarly, those mice treated with anti-CTLA-4 and Doxorubicin combination therapy, fared significantly better than those mice treated with anti-CTLA-4 monotherapy [22]. As a monotherapy, anti-CTLA-4 was able to induce complete regression in 2 out of 10 CT-26 tumor challenged mice. As a combination therapy with Doxorubicin, anti-CTLA-4 induced the complete regression and the recovery of 9 out of 10 tumor challenged mice [22]. Additionally, of those mice receiving

both Doxorubicin and a checkpoint inhibitor, a higher degree of efficacy was observed in immunocompetent mice than in immune incompetent mice [22]. This suggests that the use of Doxorubicin resulted in the generation or enhancement of an adaptive immune response.

From these data, it is reasonable to assume that administering Doxorubicin in conjunction with Val-boroPro in Balb/c mice inoculated with the CT-26 mouse cancer cell line, will result in a more effective anti-cancer immune response than that which could be mounted from Val-boroPro alone, as these data suggest that Doxorubicin is, in effect, turning a non-antigenically visible cancer into a cancer that can be recognized by the adaptive immune system by increasing the cancers antigenic stimulus. Additionally, the mechanism of Val-boroPro is similar to that of a checkpoint inhibitor with respect to its anti-cancer activity. Thus, it is hypothesized that administering Doxorubicin in addition to Val-boroPro in a syngeneic cancer model, such as the CT-26 model, will provide the dendritic cells in the tumor microenvironment with recognizable tumor-associated antigens, and that the addition of Doxorubicin will therefore facilitate the activation of the adaptive immune system, and will result in the generation of T-cell associated anti-cancer immunity.

1.6 Xaa-boroPro's and the discovery of the DASH Family

Val-boroPro (VbP) was first synthesized in the 1990s at Tufts University's Sackler School of Graduate Biomedical Sciences in the Bachovchin Lab. Its intended purpose at the time of its synthesis was to investigate the biological function of DPP4. Inhibition of DPP4 by Val-boroPro was found to have anti-diabetic effects, and DPP4 was later validated as a clinical target for antidiabetic therapy.

In addition to its antidiabetic effect, preclinical work with Val-boroPro was found to induce anticancer activity across a variety of mouse models [7]. This anticancer activity was not observed with inhibitors specific for DPP4 [2]. The anticancer activity stimulated by treatment with Val-boroPro was first identified following the discovery of DPP4 independent hematopoietic activity via the upregulation of hematopoietic growth factors [2]. DPP4's independence raised the need to reassess the pharmacological targets of Val-boroPro, leading to the realization that DPP4 is a member of subfamily of related serine proteases referred to as the DASH family of DPP4 structural activity homologs.

DASH family proteins are classified and clustered on the basis of gene sequence irrespective of their enzymatic activity. Generally, references to the DASH family exclude those enzymes that lack enzymatic activity, as those enzymatically inactive DASH family members are not interesting as therapeutic targets. The DASH family proteases are DPP2 (also called DPP7), DPP4, DPP8, DPP9, FAP, and PREP, and any reference made to the DASH family will be exclusive to these proteolytic DASH family members. Figure 1.3 is a summary of the DASH family members, and their respective biological activities.

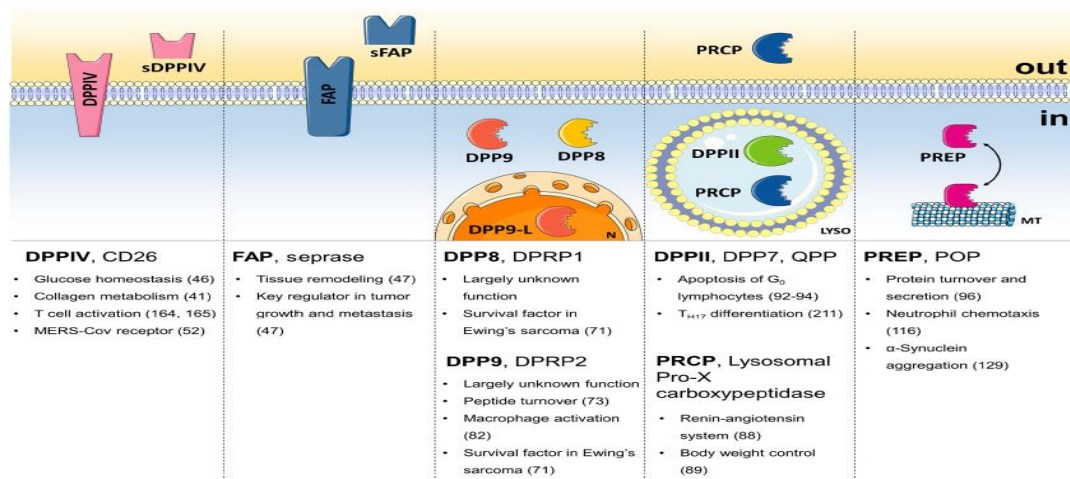


Figure 1.3. DASH Family Overview

Within the DASH family, DPP2, DPP4, DPP8, DPP9, FAP and PREP share remarkably similar active sites and substrate specificity, and each of these enzymes is an inhibitory target of Val-boroPro with varying degrees of affinity.

1.7 DASH Substrate Specificity

DASH Serine proteases are members of the α/β -hydrolase family and each possess a Serine nucleophile and a catalytic triad [4]. These DASH family enzymes are defined by the primary sequence of the amino acids that make up their cleavage motifs, which are ordered Serine, Aspartic Acid, Histidine [5]. The configuration of these amino acids within the folded tertiary structure of the active site is varied between DASH family members [5].

Among the DASH family of enzymes, DPP2, DPP4, DPP8, DPP9, and FAP share an exopeptidase activity that cleaves dipeptides from the amino-terminus of peptides after proline. Thus, each of these enzymes recognize Val-boroPro as a transition state analog. Additionally, within the DASH family, FAP and PREP exhibit endopeptidase activities that are proline dependent [5].

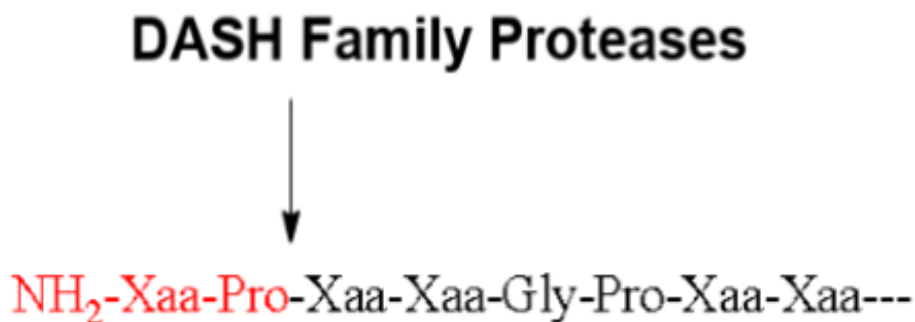


Figure 1.4. DASH Family Specificity

The known implications of Proline-cleaving enzymes have given rise to the proline checkpoint hypothesis [4]. The proline checkpoint hypothesis speculates that enzymes

which cleave after proline may serve in a regulatory capacity. The function of DPP4 in regulation of glucose metabolism via its proteolytic inactivation of GLP-1 provides the prototypical example of the proline checkpoint hypothesis [4]. Val-boroPro's suspected anticancer mechanism aligns with this hypothesis with respect to the governance of the immune system.

1.8 Val-boroPro's Anticancer Mechanism of Action

The current understanding of the anticancer mechanism of action of Val-boroPro comes from both in vivo studies in tumor models and in vitro studies in cell culture systems.

In vivo, Val-boroPro induces specific T-cell anticancer immunity and T-cell-independent anticancer activity via the stimulation of cytokine and chemokine production in Balb/c mice inoculated with MM46T fibrosarcoma cells, as measured by mRNA expression. [7, 8]

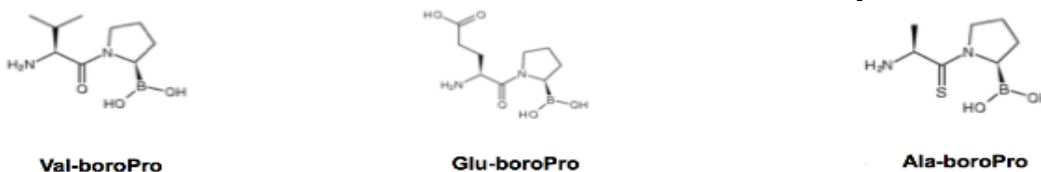
The induction of these cytokines and chemokines revealed IL-1 β signaling to be a critical feature of the anticancer immune response triggered by Val-boroPro [8]. In vivo, this was demonstrated by KO mice that lacked a type-1 IL-1 receptor, and failure to release these critical cytokine and chemokines [20]. Thus, the IL-1 β pathway was elucidated as the critical pathway responsible for Val-boroPro's induction of cytokine and chemokine production in vivo.

To isolate the cellular site responsible for IL-1 β induction, in vitro work was performed utilizing the THP-1 human monocyte cell line [21]. In vitro, it was shown that the THP-1 cells respond to proinflammatory signals derived from bacteria with the release of IL-1 β [21]. Additionally, the induction of IL-1 β production by THP-1 cells was

shown to be significantly stimulated by treatment with Val-boroPro [21]. These results suggest the monocyte is the cell responsible for IL-1 β induction by Val-boroPro [21]. After identifying the cellular site of IL-1 β induction, Val-boroPro's anticancer dependence on an intact IL-1 β pathway was again confirmed, this time in vitro.

In vitro work in a human monocyte co-culture system demonstrated the either the addition of an IL-1-receptor-blocking antibody, or the addition of the IL-1R antagonist, resulted in a reduced level of mature IL-1 β released into monocyte culture supernatants as measured by Eliza [21]. The significance of IL-1 receptor signaling in the induction of IL-1 β was also confirmed in vitro by western blot, which captured the levels of pro-IL-1 β released by monocytes harvested from the same set of cultures [21]. It was found that co-stimulation with Val-boroPro resulted in a dramatic increase in intracellular pro-IL-1 β levels. This was attenuated when the IL-1 receptor antagonist, Kineret, or an anti-IL-1 receptor antibody was introduced to the cellular culture system [21].

Table 1.1. Xaa-boroPro IC₅₀ Values for DASH Family Members



IC₅₀, nM

	DPP IV	DPP8	DPP9	PREP	DPP II	FAP
Val-boroPro	1.0	4.0	2.0	35	21	17
Glu-boroPro	1.0	20.0	13	340	12	4.0
Ala-boroPro	5.0	4.0	2.0	440	2.0	130

Advances in knowledge of Val-boroPro's molecular target(s) and its molecular mechanism for the induction of IL-1 β began with an investigation of the Val-boroPro in

cellular culture systems to test and eliminate all of the potential inhibitory target(s) responsible for its anticancer activity [21]. In a purified enzyme system, IC₅₀'s for Val-boroPro and its closely related analogs, Glu-boroPro and Ala-boroPro were obtained for DPP2, DPP4, DPP8, DPP9, FAP and PREP [21]. These values are given in table 1.1 [21].

To determine the molecular site of IL-1 β induction, FAP and DPP4 were eliminated from the list of potential anticancer inhibitory targets of Val-boroPro, as the induction of IL-1 β is controlled by macrophages and monocytes, thus, Val-boroPro's target was presumed to be born on a cell of the monocyte/macrophage lineage [21]. Exploration of DPP2 by the Bachovchin lab in cellular culture systems showed its isolated inhibition stimulated the induction of IL-17, but not the induction of IL-1 β , and it was therefore dismissed as the inhibitory target responsible for Val-boroPro's anticancer activity.

To eliminate DPP8 and DPP9 inhibition as the source of IL-1 β induction, derivatives of isoindoline were used to inhibit DPP8 and DPP9, as isoindolin derivatives are selective and potent inhibitors of DPP 8 and 9[21]. When isoindoline derivatives were added to cultures of PMA-differentiated THP-1 cells in the presence Val-boroPro, it resulted in the induction of IL-1 β , as was determined by ELISA of culture supernatants [21].

Later, the activation of IL-1 β induction resulting from treatment with Val-boroPro, was shown to proceed via the activation of caspase-1 [21]. This was discovered as THP-1 cells incubated with the isoindoline derivative and assayed for caspase-1 activity, observed a dose- and time-dependent increase in caspase-1 activity following treatment with Val-boroPro [21]. The time course of caspase-1 activation emulated that of IL-1 β

secretion [21]. From this in vitro work, it was elucidated that in cells of the monocyte or macrophage lineage, the inhibition of DPP8, DPP9, or both, is responsible for the IL-1 β induction that follows treatment with Val-boroPro [21]. As “the inhibition of DPP 8 [and DPP]9 appears to trigger the conversion of the inactive caspase-1.... into the active form responsible for processing pro-IL-1 β into mature, biologically active IL-1 β ” [21].

1.9 Expanded mechanistic Understanding of Val-boroPro Anticancer Mechanism

Recent work has expanded upon the mechanistic understanding of IL-1 β induction by Val-boroPro. The use of CRISPR gene editing by the Dan Bachovchin lab has elucidated that upon its inhibition in macrophages, DPP8 and DPP9 set off an intracellular cascade that results in pyroptosis [12,13]. Pyroptosis induced by Val-boroPro has been shown to proceed through the monocyte/macrophages’ s NLRP1 inflammasome (CARD8 in humans), Caspase 1, and Gasdermin D [12,13]. These results have been confirmed by Zhong et al [14] and de Vasconcelos et al [15].

Pyroptosis induced by Val-boroPro and its analogs have consistently demonstrated more profound anticancer in immunogenic cancer models [17]. This observation reconciles with assay work done by Point Therapeutics, which found that following Val-boroPro induced pyroptosis in macrophages and monocytes, there is a release of IL-1 β and IL-18. Both of these cytokines have been implicated in the activation of T-cell dependent immune responses, leading to the hypothesis that the induction of IL-1 β and IL-18 in macrophages drives the antitumor T-cell response produced by Val-boroPro in tumor-challenged mice [21].

This aligns with data generated by Point Therapeutics, which found that Val-boroPro's anticancer activity was significantly weakened in mice that were deficient in the T cell receptor [21].

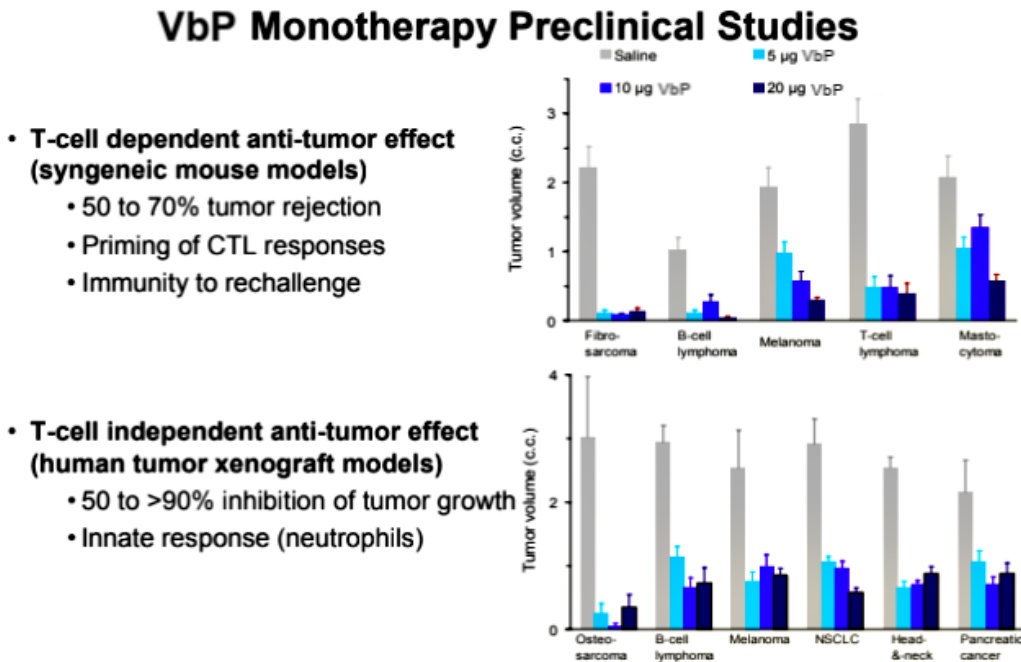


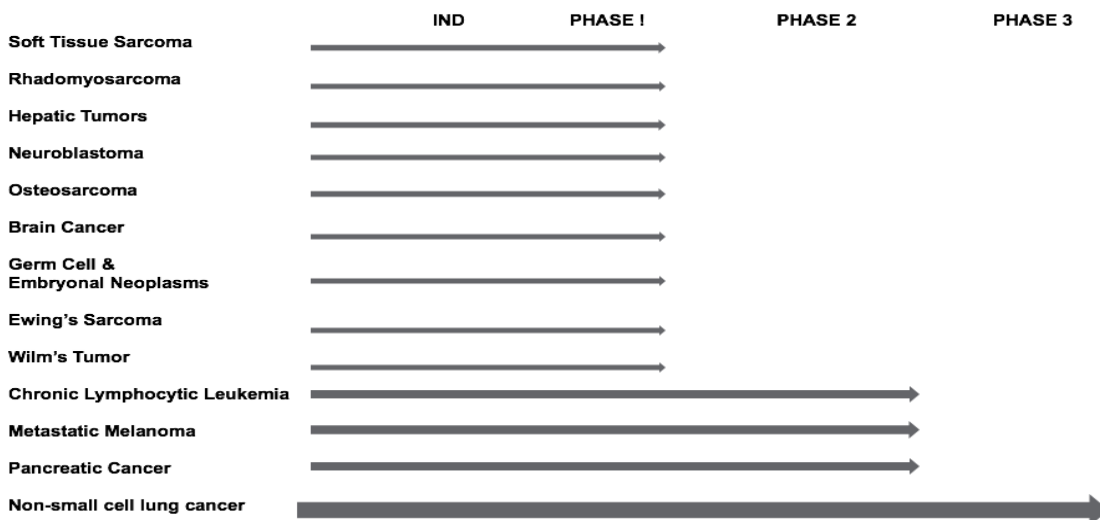
Figure 1.5. Val-boroPro T-cell Dependence

As shown in figure 1.5, which was generated by Point Therapeutics, in tumor-challenged mice, Val-boroPro activates a T-cell mediated responses against a number of non-syngeneic tumors [21]. In the absence of an activated T cell response, the antitumor activity generated by Val-boroPro is greatly diminished [21]. The results of these experiments imply that effective T cell engagement is an essential components of the tumor regression and rejection observed with Val-boroPro, and this data confirms the adaptive immune system as a critical component of the anticancer immune response generated from treatment with Val-boroPro, and Val-boroPro's reliance on the presence of a detectable antigen in order for its full anticancer activity to be harnessed.

1.10 Val-boroPro's Clinical History

In 2004, Val-boroPro received fast track designation as an early immune-oncology agent. It filed INDs for a variety of indications, but discontinued its programs for soft tissue sarcoma, rhabdomyosarcoma, hepatic tumors, neuroblastoma, osteosarcoma, brain cancer, germ cell and embryonal neoplasms, Ewing's sarcoma, and Wilm's tumor following phase 1 of clinical trials. Val-boroPro progressed to phase 2 clinical trials as a single agent therapy for metastatic melanoma, phase 2 clinical trials as a combination therapy for pancreatic cancer, chronic lymphocytic leukemia and metastatic melanoma, and it progressed to phase 3 clinical trial as a combination therapeutic agent for non-small cell lung cancer. In total, during its time as a clinical candidate, Val-boroPro was administered to more than 500 human patients ranging from Phase 1 to phase 3 clinical trials.

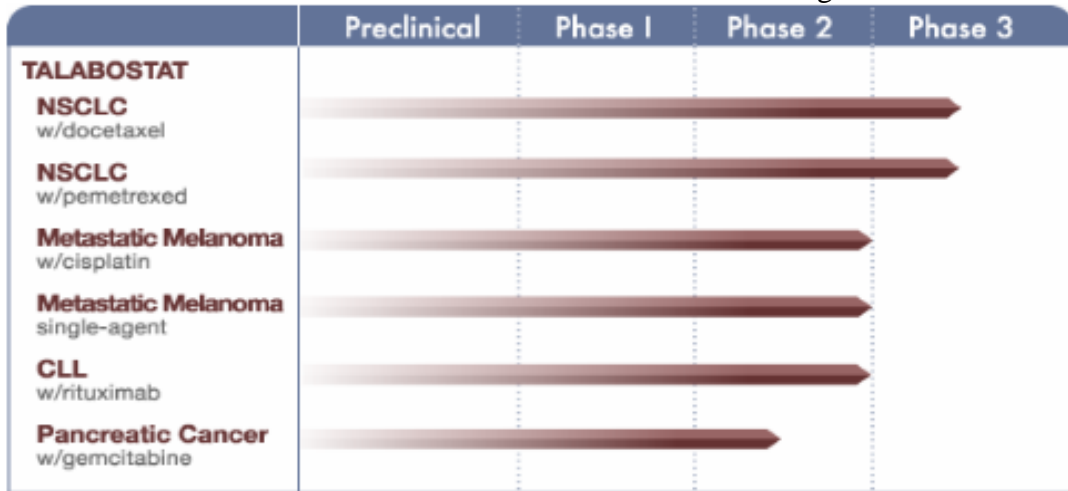
Table 1.2 Val-boroPro Clinical Indications



Examination of the clinical programs with Val-boroPro that advanced beyond phase one reveals that none of the combination therapeutic discourses coupled Val-boroPro

treatment with an agent thought to be immunogenic or to have any beneficial immunologic activity. Instead, it is believed that the agents which were given in combination trials with Val-boroPro, would have immunosuppressive effects [1] which likely handicapped, not enhanced the effects of Val-boroPro.

Table 1.3. Val-boroPro Phase 2 and 3 Clinical Programs



In 2007, Val-boroPro failed to generate efficacy data to meet the standards required to obtain clinical approval. Additionally, its toxicity data resulted in it being placed on FDA clinical hold. These toxicities resulted in a non efficacious concentration of Val-boroPro being administered throughout the aforementioned trials.

1.11 Elucidating the Mechanism of Val-boroPro Toxicities

Following its phase 3 clinical failure, much exploration has been done to determine the etiology of Val-boroPro induced toxicities, which was discovered to be its induction of an eicosanoid storm. Subsequently, efforts turned to methods to mitigate the eicosanoid induced toxicities.

In 2018 the FDA lifted its clinical hold on Val-boroPro, and it is now being tested in phase 1 clinical trials for pancreatic cancer as a combination therapy with a PDL-1.

Val-boroPro was permitted to reenter clinical trials due to the hypothesis that co-therapy

with an anti-PDL-1 will allow for a lower dose of Val-boroPro to be administered, as it will work synergistically with Val-boroPro's mechanism of action to generate a more efficacious immune response at a nontoxic concentration.

In addition to the promise of increased efficacy from a combination therapy, the exploration of the mechanism of Val-boroPro's underlying toxicity revealed PGE₂ induction to a critical step in the generation of the eicosanoid storm. Thus, through the use of COX inhibitors to suppress PGE₂, the Bachovchin lab has been effective at offsetting the previously dose constraining toxicities experienced with Val-boroPro and has prevented hypovolemia and edema in both mouse and rat models. This should allow for a dose higher than that administered during the failed phase 3 trial to be safely administered to human patients.

1.12 Experimental Rationale & Doxorubicin as an Immunogenic Chemotherapeutic Agent

The current therapeutic concept of boosting endogenous immunity to produce clinically relevant tumor response is based on the finding that many tumors appear to stimulate a T-cell-mediated immune response against tumor antigens, but the response is insufficient to provide clinical benefit due to the many immunosuppressive protections implemented by the tumor to hinder the immune system in providing a clinically relevant tumor response [1].

Certain chemotherapeutic agents have the capacity to increase tumor immunogenicity and thereby increase T-cell priming against tumor antigens. Such agents are referred to as immunogenic chemotherapy [18]. Immunogenic chemotherapy is

defined operationally as chemotherapeutic agents that not only kill tumor cells but are more effective in immunocompetent than in immunodeficient mice [18].

The components of immunogenic tumor cell death that stimulate the maturation of dendritic cells into mature-antigen presenting cells that process tumor antigens and more efficiently prime tumor antigen-specific T cells, including cytotoxic CD8+ T cells is summarized below.

In cancer cells undergoing immunogenic cell death, calreticulin (CRT) translocates to the cell surface, and ATP and high mobility group box 1 (HMGB1) protein are released into the tumor microenvironment. Cognate interactions between these molecules and receptors present on the surface of immature dendritic cells signal their recruitment to the tumor microenvironment, and the engulfment of tumor antigens and their presentation to T cells [18].

1.13 Chapter 1 notes

The tables and figures provided throughout chapter 1 of this master's thesis were primarily generated by the Bachovchin lab and the companies that were predicated on its intellectual property, Arisaph Pharmaceuticals and Point Therapeutics. These figures and tables and their origins are referenced in the text immediately surrounding them, and include figures 1.1, 1.2, 1.3, 1.4, 1.5, and tables 1.1 and 1.3. No figures or tables were taken from published work.

Chapter 2. Materials and Methods

2.1 Animals

Balb/c female mice were purchased from Charles River Laboratories in Willimington, MA and arrived at the DLAM facility at 7 weeks of age. Mice were feed a diet of standard mouse chow (Teklad) and were given continual access to clean drinking water, which was augmented with Acetaminophen on an ongoing basis when mice presented with tumor necrosis and/or ulceration. Mice were housed in cages of 5 mice per cage and were kept in the DLAM facility at Tufts University Sackler School of Graduate Biomedical Sciences. All animal experiments were done in compliance with institutional guidelines for animal care and were approved by the institutional Animal Care and Use Committee.

2.2 Tumor Cell Line and *in vitro* Culture

Mouse colon cancer cells cultured from chemically induced tumors in Balb/c mice (CT-26) were purchased from American Type Culture Collection, in Manassas, VA. CT26 cells were cultured in RPMI1640 medium, which was supplemented with 10% heat inactivated FBS purchased from Atlanta Biologicals, in Lawrenceville, GA, and 1% Pen-Strep purchased from Mediatech in Manassas, VA. CT26 cells were stored at 37° C in an incubator of 5% CO₂ to provide a humidified atmosphere. Cells were sub-cultured three times per week.

2.3 Therapeutic Agents and Formulation

Therapeutic agent Val-boroPro, L-valinyl-L-boroproline, USAN talabostat, was synthesized in the Bachovchin lab at Tufts University Sackler School of Graduate Biomedical Sciences as a crystalline solid by Jack Lai and Wegen Wu and was found to

have a purity level of $\geq 98\%$ as measured by HPLC. The ID-lot number for this compound was 2054-14.

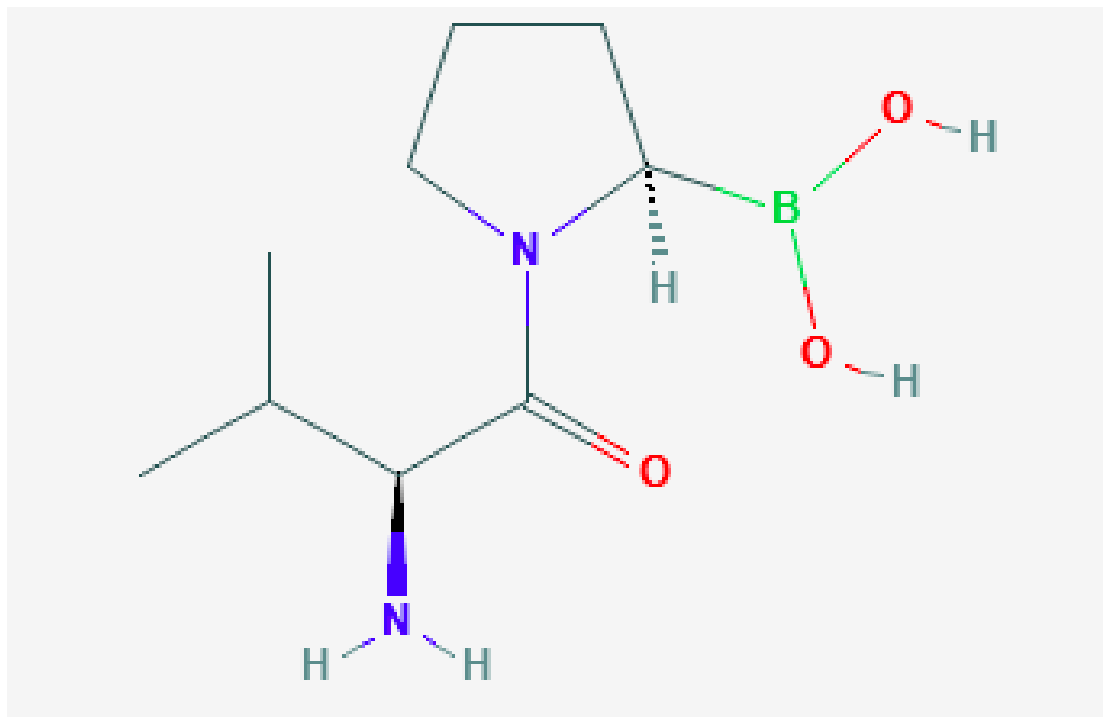


Figure 2.1. Val-boroPro

Val-boroPro's synthesis was carried out in accordance with the synthetic scheme and methods outlined in USPTO patent US4935493A "Protease Inhibitors." The material provided from this synthesis was weighed and dissolved at the appropriate concentration in pH 2 water (0.01 N HCl). The concentration was 0.1 mg/ml. This dosing solution of Val-boroPro was prepared in aliquots of 10 X 5 ml was stored frozen at -20°C until used.

Doxorubicin was obtained through DLAM from the Tufts Medical Center Pharmacy, which procured the injectable formulation of Doxorubicin, Doxorubicin Hydrochloride Injection, from Fresenius Kabi as a USP grade compound with Doxorubicin concentration of 2mg per mL. Doxorubicin Hydrochloride was stored at 4°C until used.

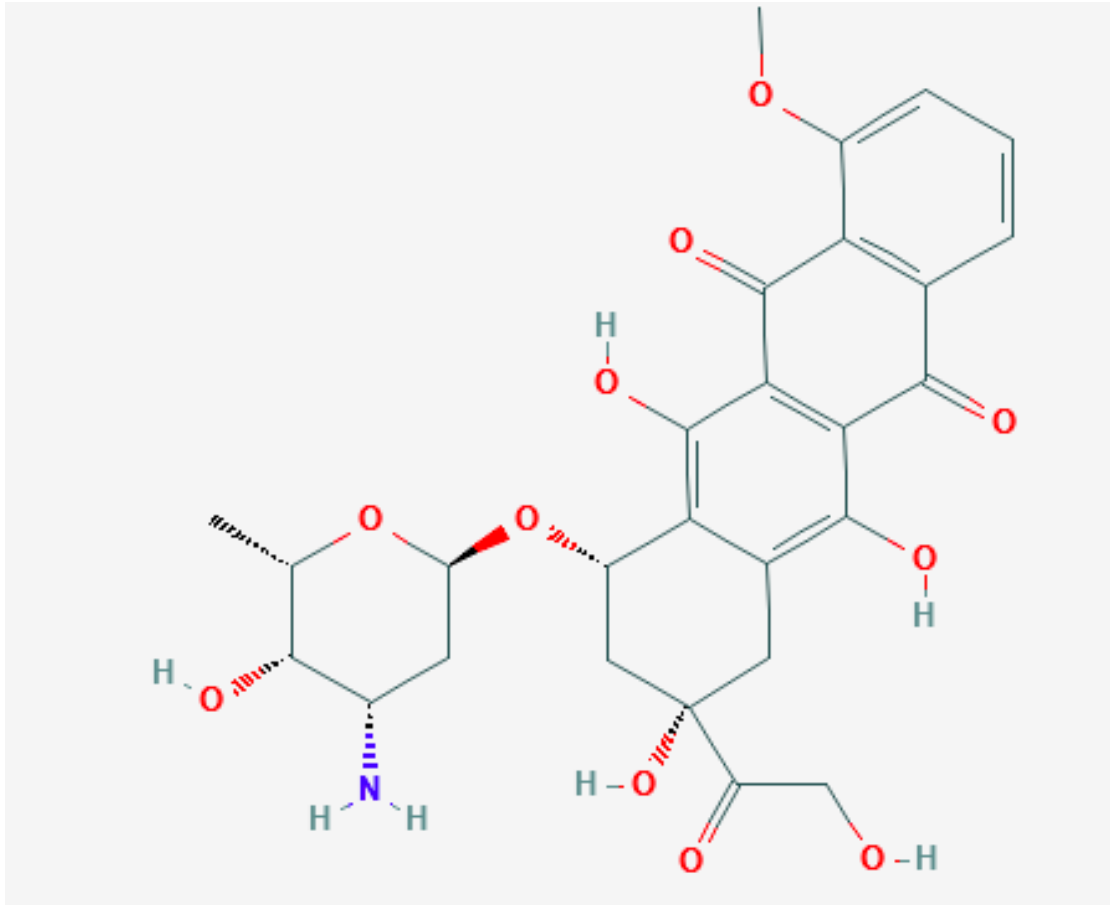


Figure 2.2. Doxorubicin

On the day of injection, the doxorubicin was diluted to 2 μM (0.001088 mg/ml) as follows: 0.01 mL of 2 mg/mL Doxorubicin added to 0.174 mL sterile phosphate buffered saline (PBS). Then 0.15 mL of the first dilution was added to 1.35 mL sterile PBS for a total dilution of 1840x. 0.05 mL of 2 μM Doxorubicin was injected into the tumor. Diluted doxorubicin was used on the same day as the dilution.

2.4 Tumor Inoculation and Protocol

One hundred Balb/c mice were inoculated with Balb/c derived CT26 cells colon cancer cells eight days after arriving at the DLAM facility. Each Balb/c mouse was inoculated subcutaneously at the right shoulder with 1×10^5 CT26 cells/mouse suspended

in .2 ml of PBS. Following inoculation, mice were monitored 3 times per week, where their tumor size and body weights were taken and recorded.

2.4.1 Group Assignments

Of the 100 mice inoculated with CT26 cells, 40 mice with the highest degree of homogeneity across tumors and body weights were selected to participate in treatment. Mice were then grouped in cohorts of 10 mice per cohort according to the animal's body weight and tumor volume. This was done to best achieve consistency across treatment groups. Mouse groupings are depicted below in table 2.1, along with each mouse's tumor volume at the time of its grouping in table 2.2. Mouse cohorts will be referenced by their letter assignments. Mouse cohort A represents the group of mice that received oral PO treatment by Val-boroPro alone. Mouse cohort B represents the group of mice that received both oral PO treatment by Val-boroPro and intertumoral injections of Doxorubicin. Mouse cohort C represents the group of mice that received only intertumoral injections of Doxorubicin, and mouse cohort D represents the vehicle cohort, which received neither treatment with Val-boroPro nor Doxorubicin.

Table 2.1 Mouse Groupings Mean Weight and Tumor Volume

<p>Group A (Val-boroPro only)</p> <ul style="list-style-type: none"> • Mouse Mean body Weight = 18.8kg • Mouse Mean Tumor Size = 82.23mm³ 	<p>Group C (Doxorubicin Only)</p> <ul style="list-style-type: none"> • Mouse Mean body Weight = 18.6kg • Mouse Mean Tumor Size = 91.20mm³
<p>Group B (Combination)</p> <ul style="list-style-type: none"> • Mouse Mean body Weight = 18.5kg • Mouse Mean Tumor Size = 76.84mm³ 	<p>Group D (Vehicle)</p> <ul style="list-style-type: none"> • Mouse Mean body Weight = 18.8kg • Mouse Mean Tumor Size = 97.36mm³

Table 2.2. Individual Mouse Tumor Volumes at the Time of Grouping

Val-boroPro			Dox		
Cage-#	Vol	Grp Mean	Cage-#	Vol	Grp Mean
1-1	37.6475	82.2297	3-5	166.698	91.19055
1-2	71.632		4-1	74.52	
1-3	127.0565		4-2	167.8875	
1-4	124.5375		5-1	140.4	
2-1	35.378		5-3	86.4	
2-3	67.4885		5-4	151.2	
2-4	86.0625		5-5	24.5	
3-1	80.4315		7-1	48	
3-2	117.975		7-2	34.3	
3-3	74.088		7-3	18	

Val-boroPro + Dox			Vehicle		
Cage-#	Vol	Grp Mean	Cage-#	Vol	Grp Mean
7-4	60.75	76.833	10-2	105.875	97.3592
7-5	75		10-3	90.75	
8-2	71.25		10-4	160.2	
8-3	42.875		11-1	162.6625	
9-1	56		11-3	56	
9-2	55.6875		11-4	126	
9-3	87.88		12-1	151.4235	
9-4	121		12-2	59.094	
9-5	142.2		12-3	28.512	
10-1	55.6875		12-4	33.075	

2.4.2 Tumor Measurements

Tumor measurements were taken beginning the day after inoculation. Tumor volumes were measured using digital calipers and measurements were recorded three times within each seven-day period, on Monday, Wednesday, and Friday. When mouse cohorts contained mice bearing an average tumor size of approximately 80-100mm³, mice began on their respective course of treatment. Tumors volumes were quantified using $Volume = (Width^2 \times Length)/2$.

Following treatment, cages were labeled identically with a hidden key that corresponded to a cage numbering system assigned by DLAM. This allowed for tumor measurements to be taken blind to the knowledge of the treatment each mouse received. The mouse tumor measurement and body weight schedule used for this experiment is given bellow.

Table 2.3. Tumor Measurement Schedule

Measurement Schedule						
M	T	W	Th	F	Sa	Su
1/7/2019	1/8/2019	1/9/2019	1/10/2019	1/11/2019	1/12/2019	1/13/2019
1/14/2019	1/15/2019	1/16/2019	1/17/2019	1/18/2019	1/19/2019	1/20/2019
	Innoculate	BW/Tvol		BW/Tvol		
1/21/2019	1/22/2019	1/23/2019	1/24/2019	1/25/2019	1/26/2019	1/27/2019
Bw/Tvol		Bw/Tvol		BW/Tvol		
1/28/2019	1/29/2019	1/30/2019	1/31/2019	2/1/2019	2/2/2019	2/3/2019
BW/Tvol		Bw/Tvol		BW/Tvol		
2/4/2019	2/5/2019	2/6/2019	2/7/2019	2/8/2019	2/9/2019	2/10/2019
BW/Tvol		BW/Tvol		BW/Tvol		
2/11/2019	2/12/2019	2/13/2019	2/14/2019	2/15/2019	2/16/2019	2/17/2019

Throughout this experiment, animals were dosed with their respective treatment over a 4-week period. During this time, body weights were used to track the health of the animal. Any animal participating in this experiment who experienced a body weight decrease to 85% of its starting weight was euthanized, per the animal care and welfare requirements set forth by IACUC. Tumor volumes were monitored with calipers 3 times per week to determine the effect of treatment on tumor growth rate, and as well as to monitor IACUC humane endpoint guidelines. Any mouse bearing a tumor size equivalent to 1,500 mm³ in volume, or that reached 2 cm in any one dimension, was scheduled for euthanasia. Additional IACUC euthanasia criteria (humane endpoints) which was monitored for throughout the study were tumor ulcerations greater than 5 mm and/or infected ulcers, prolonged labored breathing or respiratory distress observed by DLAM staff during cage changes and mouse feeding, significant abdominal distention (ascites) observed by DLAM staff, or a compromised ability to eat or drink and/or an absence of or abnormal fecal or urine output, lethargy or reluctance to move, abnormal gait, paresis or paralysis as observed by DLAM staff.

2.4.3 Drug Doses and Schedule of Administration

Once tumors had reached a volume of approximately 80-100mm³, mice were grouped to begin their respective courses of treatment.

Table 2.4. Group Treatment Schedules

Group A (Val-boroPro only)	Group C (Doxorubicin Only)
<ul style="list-style-type: none">• 1st IT injection, 50 uL, PBS given 10 days following inoculation with CT26 cells when tumors reached 40-50mm²• 2nd IT injection, 50 uL, PBS given 17 days following inoculation with CT26 cells• 20 µg PO Val-boroPro QDx5 beginning 9 days following inoculation with CT26 cells and given 5 days per week	<ul style="list-style-type: none">• 1st IT injection of 50 uL, 2 uM Doxorubicin given 10 days following inoculation with CT26 cells when tumors reached 40-50mm²• 2nd IT injection, 50 uL, 2 uM Doxorubicin given 17 days following inoculation with CT26 cells• 0.2 ml of PO pH 2.0 water QDx5 beginning 9 days following inoculation with CT26 cells and given 5 days per week
Group B (Combination)	Group D (Vehicle)
<ul style="list-style-type: none">• 1st IT injection of 50 uL, 2 uM Doxorubicin given 10 days following inoculation with CT26 cells when tumors reached 40-50mm²• 2nd IT injection, 50 uL, 2 uM Doxorubicin given 17 days following inoculation with CT26 cells• 20 µg PO Val-boroPro QDx5 beginning 9 days following inoculation with CT26 cells and given 5 days per week	<ul style="list-style-type: none">• 1st IT injection, 50 uL, PBS given 10 days following inoculation with CT26 cells when tumors reached 40-50mm²• 2nd IT injection, 50 uL, PBS given 17 days following inoculation with CT26 cells• 0.2 ml of PO pH 2.0 water QDx5 beginning 9 days following inoculation with CT26 cells and given 5 days per week

Mouse groups A and B received treatment of 20 µg by gavage Val-boroPro beginning 9 days after their inoculation with CT26 cells. This treatment was given 5 days per week at the same time each day. Mouse groups C and D received 20 µg by gavage of pH 2.0 water beginning 9 days after their inoculation with CT26 cells. This treatment was given 5 days per week at the same time each day.

On days 10 and 17 post inoculation with CT26 cells, all cohort groups (A, B, C and D) were anesthetized using 3-5% inhalable isoflurane. While anesthetized, groups B and C received intertumoral injections of 50 uL, 2 uM Doxorubicin, while groups A and D received intertumoral injections of 50 uL, PBS.

A schedule of inoculation and treatment for the animals involved in this study is given in table 2.5.

Table 2.5. Inoculation and Dosing Schedule

Inoculation and Dosing Schedule						
M	T	W	Th	F	Sa	Su
1/7/2019	1/8/2019	1/9/2019	1/10/2019	1/11/2019	1/12/2019	1/13/2019
1/14/2019	1/15/2019	1/16/2019	1/17/2019	1/18/2019	1/19/2019	1/20/2019
	Innoculate					
1/21/2019	1/22/2019	1/23/2019	1/24/2019	1/25/2019	1/26/2019	1/27/2019
			VbP	VbP + DOX	VbP	VbP
1/28/2019	1/29/2019	1/30/2019	1/31/2019	2/1/2019	2/2/2019	2/3/2019
VbP	VbP	VbP	VbP	VbP + DOX		
2/4/2019	2/5/2019	2/6/2019	2/7/2019	2/8/2019	2/9/2019	2/10/2019
VbP	VbP	VbP	VbP	VbP		
2/11/2019	2/12/2019	2/13/2019	2/14/2019	2/15/2019	2/16/2019	2/17/2019

2.5 Statistical Analysis

Mean tumor volumes, mean mouse body weights and standard error of the mean were calculated. Statistical significance between control and different treatment groups was determined by ANOVA using Graft Pad Prism software.

2.6 Chapter 2 notes

None of the figures or tables contained in chapter 2 were generated by an external party. All tables and figures contained in this chapter are the work of the thesis author.

Chapter 3. Results

3.1 Tumor Size

The effect of Doxorubicin and Val-boroPro co-therapy on tumor size was compared against the effect of Val-boroPro or Doxorubicin monotherapy, and against those mice that received no therapeutic treatment. Shown in figure 3.1 are graphical divergences in tumor size by treatment group with day 0 representing the day mice were inoculated with CT26 cells.

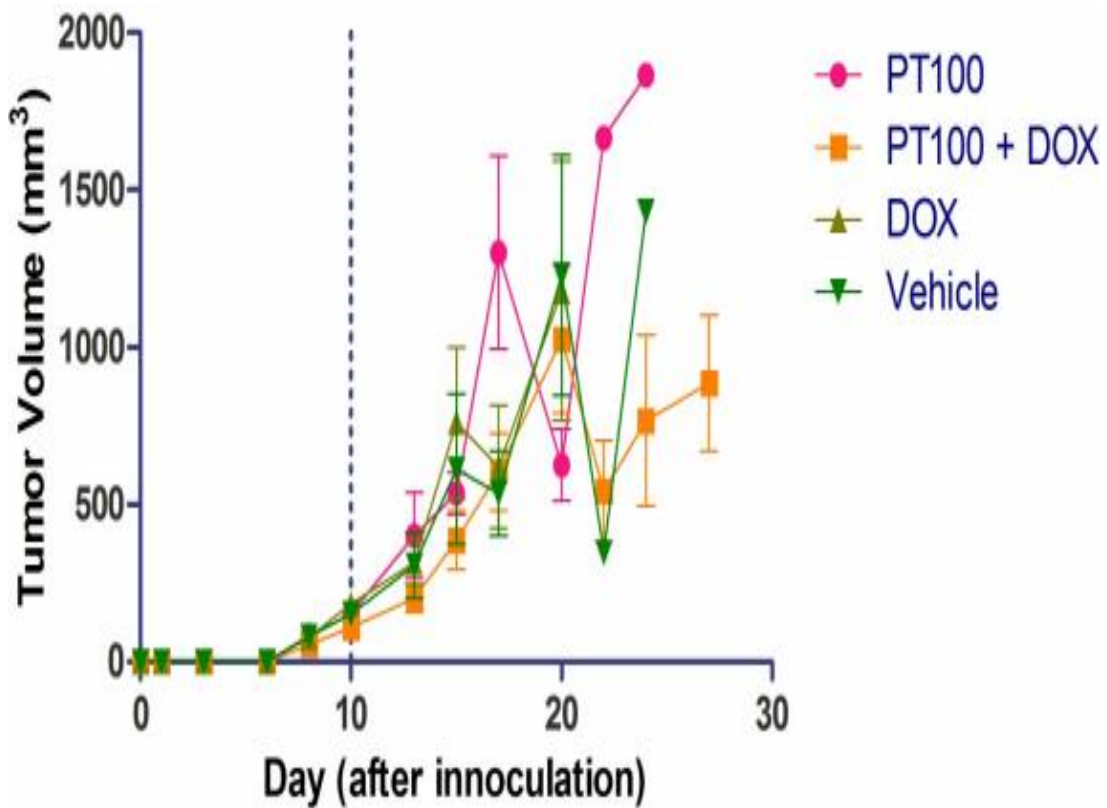


Figure 3.1. Aggregated Tumor Volumes by Treatment

As is seen in figure 3.1, combination treatment with Val-boroPro and Doxorubicin, mice appeared optically to have a slightly better prognosis than those mice

in other cohorts, however this optical divergence is not seen until 23 days after tumor inoculation and was not found to be statistically significant as the majority of mouse participants in each cohort had perished by this time. Figure 3.2 is a breakdown of each individual treatment cohort depicting the trend in individual mouse tumor burdens and the data corresponding to each mouse's tumor volume.

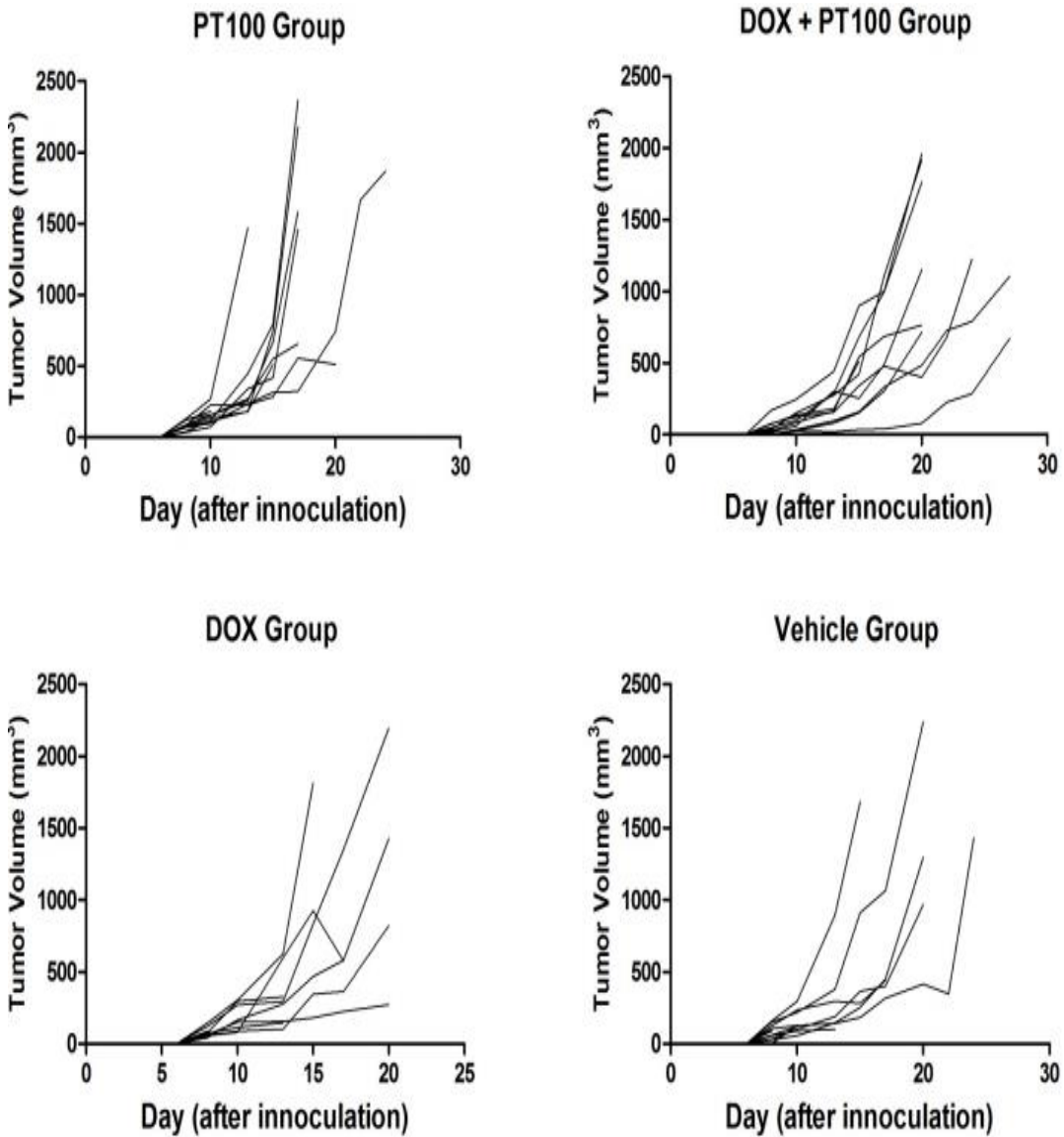


Figure 3.2 Mouse Tumor Volumes Broken Out by Group

Table 3.1 Tumor Volumes by Mouse

TUMOR VOLUMES																					
Group A											Group B										
Day	M1	M2	M3	M4	M5	M6	M7	M8	M9	M10	Day	M1	M2	M3	M4	M5	M6	M7	M8	M9	M10
0	0	0	0	0	0	0	0	0	0	0	0	0	0	0	0	0	0	0	0	0	
1	0	0	0	0	0	0	0	0	0	0	0	0	0	0	0	0	0	0	0	0	
3	0	0	0	0	0	0	0	0	0	0	0	0	0	0	0	0	0	0	0	0	
6	0	0	0	0	0	0	0	0	0	0	0	0	0	0	0	0	0	0	0	0	
8	38	72	127	125	35	67	86	80	118	74	8	38	75	168	0	0	0	25	48	34	18
10	117	111	267	156	71	97	154	227	182	137	10	111	123	244	34	28	28	85	100	151	61
13	446	182	1470	270	338	234	254	228		180	13	182	158	441	97	20	80	163	287	275	303
15	792	745		550	417	316	668	284		510	15		340	898	159	34	153	541	680	419	253
17	2363	2176		656	1458	321	1580	555			17		478	1000	331	38	304	684	996	1105	488
20						740		511			20		402	1960	485	78	714	764	1764	1918	1150
22						1665					22		678		725	227					
24						1866					24		1222		791	286					
27											27										
29											29										
31											31										
34											34										
Group C											Group D										
Day	M1	M2	M3	M4	M5	M6	M7	M8	M9	M10	Day	M1	M2	M3	M4	M5	M6	M7	M8	M9	M10
0	0	0	0	0	0	0	0	0	0	0	0	0	0	0	0	0	0	0	0	0	0
1	0	0	0	0	0	0	0	0	0	0	0	0	0	0	0	0	0	0	0	0	0
3	0	0	0	0	0	0	0	0	0	0	0	0	0	0	0	0	0	0	0	0	0
6	0	0	0	0	0	0	0	0	0	0	0	0	0	0	0	0	0	0	0	0	0
8	61	75	71	43	56	56	88	121	142	56	8	106	91	160	0	56	126	151	59	29	33
10	151	295	113	166	88	140	113	270	304	81	10	129	81	295	129	91	234	218	121	56	101
13	156	328	145	275	100			292	624	596	13	141		894		98	294	378		144	189
15	180			468	344			832	1811	925	15	182		1682			282	912		252	366
17	225			581	364			1352		576	17	317					441	1065		452	400
20	272			1425	821			2194		5100	20	413						2238		1296	968
22											22	347									
24											24	1430									
27											27										
29											29										
31											31										
34											34										

In the table 3.1, red boxes indicate the death of the mouse, either by euthanasia after reaching a human end point, or by natural causes.

P-values were calculated by ANOVA to determine the statistical significance of variations in tumor volume across treatment cohorts. Variations between cohorts A, B, C with respect to tumor volume were found to be statistically insignificant. All treated mouse cohorts had statistically significant variations in tumor volume when compared to the untreated vehicle cohort. Measurements were tested for statistical significance at days

10, 13, 15 and 17, with day 0 representing the day of inoculation with CT26 cells. After day 17, not enough mice remained in each cohort to generate meaningful statistics with respect to the relative efficacy of each treatment.

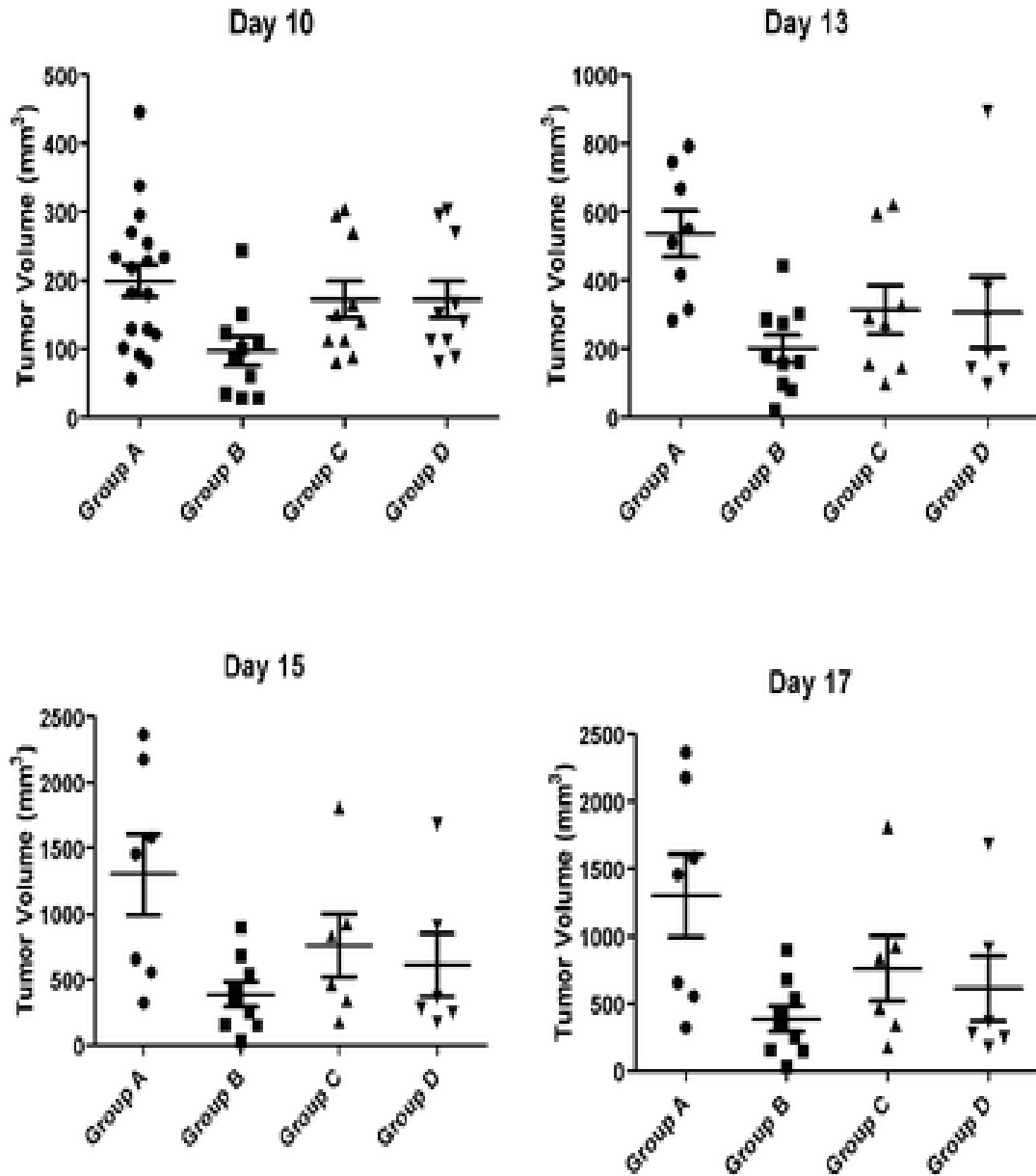


Figure 3.3. Statistical Comparison of Tumor Volume

3.2 Body weights

Mouse body weights by treatment groups did not diverge optically across treatment groups until 15 days following tumor inoculation. Beginning at day 15, the untreated vehicle group maintained a higher body weight than those groups receiving a therapeutic treatment, but body weights remained consistent across treatment groups irrespective of which therapeutic treatment regimen the mice were administered. Figure 3.4 is a graphical depiction of body weights aggregated by treatment group and a raw data corresponding to each mouse body weight over time.

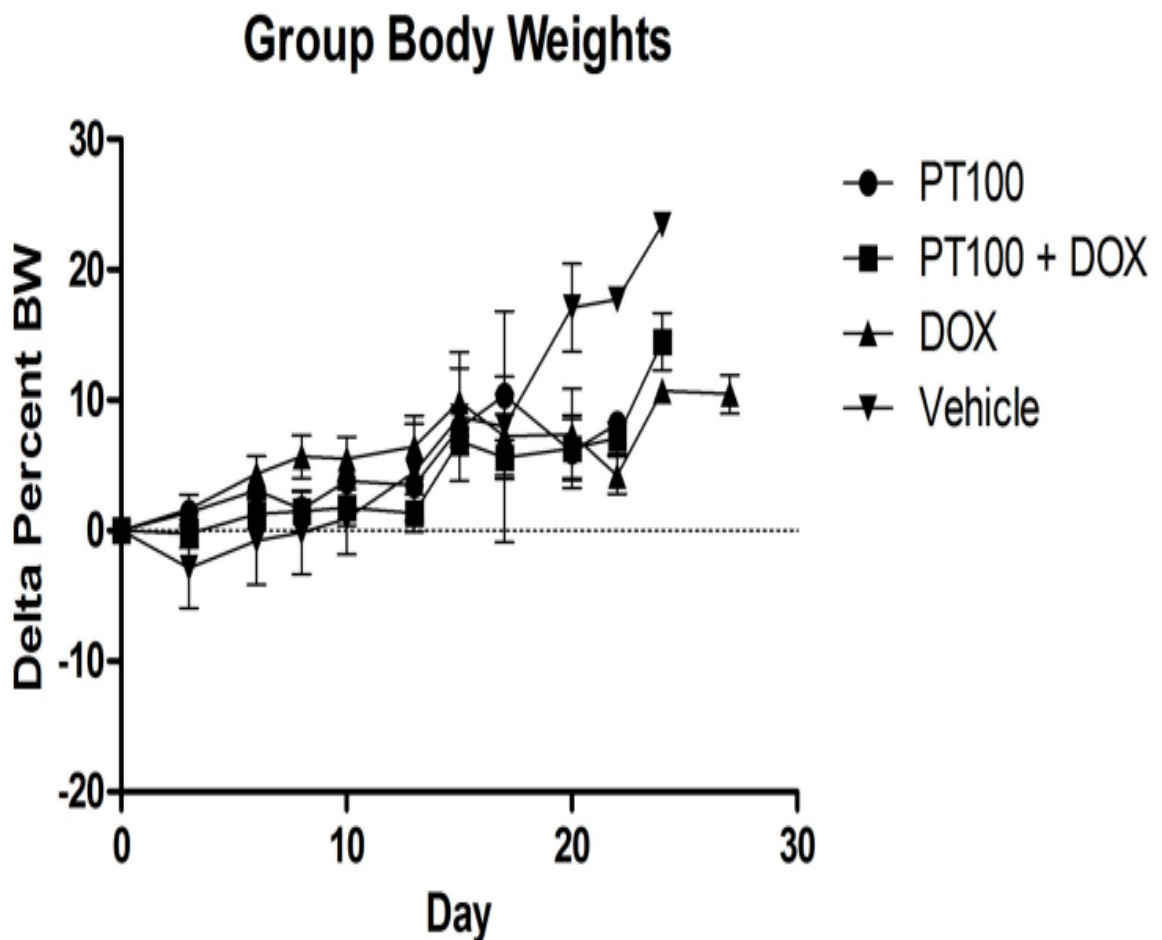


Figure 3.4 Mouse Body Weights by Group

Table 3.2 Mouse Body Weights

BODY WEIGHTS																					
Group A						Group B															
Day	M1	M2	M3	M4	M5	M6	M7	M8	M9	M10	Day	M1	M2	M3	M4	M5	M6	M7	M8	M9	M10
0	17	17	17	17	19	18	19	18	18	19	0	18	19	20	17	17	18	19	16	18	18
1	17	18	18	17	19	18	19	18	18	19	1	17	18	19	16	18	18	19	16	17	18
3	17	18	18	17	19	18	19	19	19	19	3	19	19	19	16	19	18	20	16	18	19
6	17	17	18	16	19	18	19	19	19	19	6	19	19	19	17	19	18	20	17	17	19
8	17	18	18	17	19	19	19	20	19	20	8	18	19	20	17	19	18	20	17	17	19
10	17	18	19	17	20	18	20	19	19	19	10	17	19	20	17	19	18	19	17	18	19
13	18	19		19	21	19	21	19		19	13	16	20	21	18	19	19	20	18	19	20
15	18	20		18	22	19	21	19			15		19	22	18	18	19	19	18	19	20
17						19		20			17		19	23	17	17	19	19	17	19	20
20						20					20		20			20					
22											22		21			21					
24											24										
27											27										
29											29										
31											31										
34											34										

Group C						Group D															
Day	M1	M2	M3	M4	M5	M6	M7	M8	M9	M10	Day	M1	M2	M3	M4	M5	M6	M7	M8	M9	M10
0	18	17	17	17	18	17	17	18	17	17	0	19	19	17	18	17	18	20	19	18	19
1	18	17	17	18	17	18	17	17	18	18	1	19	19	18	19	20	17	17	18	17	18
3	19	18	18	19	17	19	18	18	19	19	3	18	19	18	19	21	18	18	18	17	18
6	19	18	17	19	18	19	18	18	19	19	6	18	18	18	19	20	18	18	18	17	18
8	19	18	17	19	18	20	18	18	19	18	8	17	17	18	20	19	18	17	18	17	18
10	19	19	18	19	17	20	18	18	19	19	10	17	17	19	19	18	18	18	18	19	17
13	19		19	20	18		19	18	18	20	13	16		20	20	18	19	18		18	
15	18		19	20	18		19	18	17	19	15	17		20	20		18			17	
17	17		19	20	18		20	18		17	17	17		21	20			17			
20					19			18			20	17			21			17			
22					20			20			22	17			22						
24					20			19			24	16									
27											27										
29											29										
31											31										
34											34										

3.3 Survival Time

With respect to survival time and life expectancy following CT26 inoculation, there was a significantly improved prognosis for those mice receiving a therapeutic treatment regime as compared to the vehicle cohort. However, there was not a significant divergence in survival time between treatment cohorts, with group A experiencing an average survival time of 19.1 days following tumor inoculation, group C surviving an

average of 20.8 days following tumor inoculation and groups C and D surviving an average number of 21.6 days and 15.4, respectively.

Optically, mouse survival data tended to favor the combined treatment cohort, group B. However, the degree of difference in survival time was not found to be statistically meaningful when compared to other treated cohorts. Figure 3.5 is a survival curve and the corresponding data regarding survival time, cause of death.

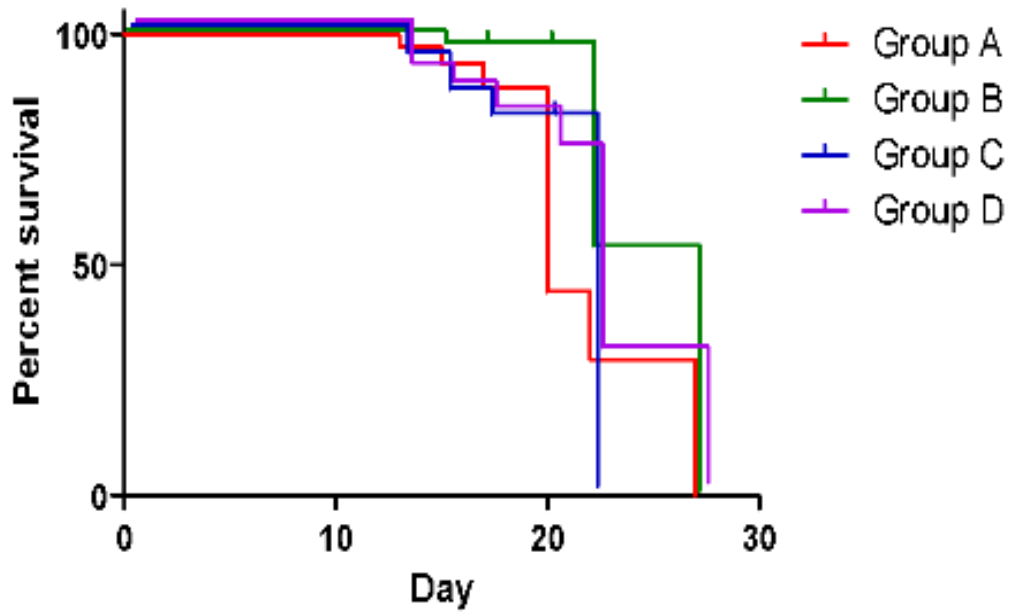


Figure 3.5. Mouse Survival Curve

3.4 Chapter 3 notes

None of the tables or figures displayed in chapter 3 of this thesis were the creation of an external party. All tables and figures in this chapter were exclusively the work of the author of this thesis.

Chapter 4. Discussion

Despite the lack of increased efficacy seen with Val-boroPro and Doxorubicin combination therapy in this study, there is reason to believe that modifications to the study's design could yield more efficacious results for this therapy.

In most preclinical cancer models in which Val-boroPro is administered to animals as a form anticancer therapy, dosing begins before tumors are of a measurable size. In this study, however, treatment was delayed until tumors were of a considerable volume, as this was necessary for intertumoral doxorubicin administration. CT26 is known to be a fast growing tumor cell line, and therefore, delaying treatment until tumors were of a sizable mass may have placed unrealistic expectations on the immune system.

Doxorubicin was administered intratumorally instead of systemically for ease of administration and to concentrate the effects of Doxorubicin within the tumor microenvironment, which sought to emulate the effects of prodrug technology developed by the Bachovchin lab to deliver Doxorubicin locally.

The Bachovchin lab designed a pro-drug which releases Doxorubicin through FAP, an enzyme expressed on malignant fibroblasts within the tumor stroma. Imaging studies conjugating this FAP releasing technology to a dye have shown that the dye was released only in the tumor microenvironment of tumor bearing animals despite being given via a systemic route of administration (oral). Conjugating this technology to Doxorubicin is expected to result in Doxorubicin's activity being concentrated within the tumor microenvironment. This transitively will allow for a higher dose of Doxorubicin to be administered with a reduced risk of toxicity [24]. For future studies, this prodrug might be given in place of intertumoral doxorubicin injections, which therefore would allow for

treatment to begin before tumors were palpable.

Additionally, future experiments should focus on the timing of treatment with Val-boroPro, as it is critical to synergize Val-boroPro dosing with Doxorubicin administration. This is due to the mechanism of both drugs, which suggest that perhaps increasing the time between chemotherapy and the start of VbP administration could optimize T cell priming and avoid any immunosuppressive effects of the chemotherapy on the activation of tumor immunity by VbP.

Chapter 5. Bibliography

1. Mellman I, Coukos G, Dranoff G. Cancer immunotherapy comes of age. *Nature*. 2011;480(7378):480-9. Epub 2011/12/24
2. Jones B, Adams S, Miller GT, Jesson MI, Watanabe T, Wallner BP. Hematopoietic stimulation by a dipeptidyl peptidase inhibitor reveals a novel regulatory mechanism and therapeutic treatment for blood cell deficiencies. *Blood*. 2003;102(5):1641-8.
3. Busek P, Malik R, Sedo A. Dipeptidyl peptidase IV activity and/or structure homologues (DASH) and their substrates in cancer. *Int J Biochem Cell Biol*. 2004;36(3):408-21
4. Rosenblum JS, Kozarich JW. Prolyl peptidases: a serine protease subfamily with high potential for drug discovery. *Current opinion in chemical biology*. 2003;7(4):496-504.
5. Edosada CY, Quan C, Tran T, Pham V, Wiesmann C, Fairbrother W, Wolf BB. Peptide substrate profiling defines fibroblast activation protein as an endopeptidase of strict Gly(2)-Pro(1)-cleaving specificity. *FEBS letters*. 2006;580(6):1581-6. Epub 2006/02/17
6. Edosada CY, Quan C, Wiesmann C, Tran T, Sutherlin D, Reynolds M, Elliott JM, Raab H, Fairbrother W, Wolf BB. Selective inhibition of fibroblast activation protein protease based on dipeptide substrate specificity. *J Biol Chem*. 2006;281(11):7437-44
7. Adams S, Miller GT, Jesson MI, Watanabe T, Jones B, Wallner BP. PT-100, a small molecule dipeptidyl peptidase inhibitor, has potent antitumor effects and augments antibody-mediated cytotoxicity via a novel immune mechanism. *Cancer Res*. 2004;64(15):5471-80.
8. Duncan BB, Highfill SL, Qin H, Bouchkouj N, Larabee S, Zhao P, Woznica I, Liu Y, Li Y, Wu W, Lai JH, Jones B, Mackall CL, Bachovchin WW, Fry TJ. A pan-inhibitor of DASH family enzymes induces immune-mediated regression of murine sarcoma and is a potent adjuvant to dendritic cell vaccination and adoptive T-cell therapy. *J Immunother*. 2013;36(8):400-11.
9. Walsh MP, Duncan B, Larabee S, Krauss A, Davis JP, Cui Y, Kim SY, Guimond M, Bachovchin W, Fry TJ. Val-BoroPro Accelerates T Cell Priming via Modulation of Dendritic Cell Trafficking Resulting in Complete Regression of Established Murine Tumors. *PLoS One*. 2013;8(3):e58860.
10. Donahue RN, Duncan BB, Fry TJ, Jones B, Bachovchin WW, Kiritsy CP, Lai JH, Wu W, Zhao P, Liu Y, Tsang KY, Hodge JW. A pan inhibitor of DASH family enzymes induces immunogenic modulation and sensitizes murine and human carcinoma cells to antigen-specific cytotoxic T lymphocyte killing: implications for combination therapy with cancer vaccines. *Vaccine*. 2014;32(26):3223-31.
11. Jesson MI, McLean PA, Miller GT, Adams S, Aubin J, Jones B. Immune mechanism of action of talabostat: a dipeptidyl peptidase targeting antitumor agent [abstract]. In: Proceedings of the 98th Annual Meeting of the American Association for Cancer Research; 2007 Apr 14-18; Los Angeles, CA. Philadelphia (PA): AACR; 2007, Abstract nr 1894.

12. Okondo MC, Rao SD, Taabazuing CY, Chui AJ, Poplawski SE, Johnson DC, Bachovchin DA. Inhibition of Dpp8/9 Activates the Nlrp1b Inflammasome. *Cell Chem Biol*. 2018;25(3):262-7
13. Okondo MC, Johnson DC, Sridharan R, Go EB, Chui AJ, Wang MS, Poplawski SE, Wu W, Liu Y, Lai JH, Sanford DG, Arciprete MO, Golub TR, Bachovchin WW, Bachovchin DA. DPP8 and DPP9 inhibition induces pro-caspase-1-dependent monocyte and macrophage pyroptosis. *Nature chemical biology*. 2017;13(1):46-53.
14. Zhong FL, Robinson K, Teo DET, Tan KY, Lim C, Harapas CR, Yu CH, Xie WH, Sobota RM, Au VB, Hopkins R, D'Oswaldo A, Reed JC, Connolly JE, Masters SL, Reversade B. Human DPP9 represses NLRP1 inflammasome and protects against autoinflammatory diseases via both peptidase activity and FIIND domain binding. *J Biol Chem*. 2018;293(49):18864-78.
15. de Vasconcelos NM, Vliegen G, Goncalves A, De Hert E, Martin-Perez R, Van Opdenbosch N, Jallapally A, Geiss-Friedlander R, Lambeir AM, Augustyns K, Van Der Veken P, De Meester I, Lamkanfi M. DPP8/DPP9 inhibition elicits canonical Nlrp1b inflammasome hallmarks in murine macrophages. *Life Sci Alliance*. 2019;2(1). Epub 2019/02/06. doi: 10.26508/lsa.201900313.
16. Halak BK, Maguire HC, Jr., Lattime EC. Tumor-induced interleukin-10 inhibits type 1 immune responses directed at a tumor antigen as well as a non-tumor antigen present at the tumor site. *Cancer Res*. 1999;59(4):911-7
17. Highfill SL, Cui Y, Giles AJ, Smith JP, Zhang H, Morse E, Kaplan RN, Mackall CL. Disruption of CXCR2-mediated MDSC tumor trafficking enhances anti-PD1 efficacy. *Science translational medicine*. 2014;6(237):237ra67.
18. Kroemer G, Galluzzi L, Kepp O, Zitvogel L. Immunogenic cell death in cancer therapy. *Annu Rev Immunol*. 2013;31:51-72.
19. Zhong FL, Robinson K, Lim C, Harapas CR, Yu CH, Xie W, Sobota RM, Au VB, Hopkins R, Connolly JE, Masters S, Reversade B. DPP9 is an endogenous and direct inhibitor of the NLRP1 inflammasome that guards against human auto-inflammatory diseases. <http://dxdoiorg/101101/260919>. 2018.
20. Apetoh L, Ghiringhelli F, Tesniere A, Obeid M, Ortiz C, Criollo A, Mignot G, Maiuri MC, Ullrich E, Saulnier P, Yang H, Amigorena S, Ryffel B, Barrat FJ, Saftig P, Levi F, Lidereau R, Nagues C, Mira JP, Chompret A, Joulin V, Clavel-Chapelon F, Bourhis J, Andre F, Delaloge S, Tursz T, Kroemer G, Zitvogel L. Toll-like receptor 4-dependent contribution of the immune system to anticancer chemotherapy and radiotherapy. *Nat Med*. 2007;13(9):1050-9.
21. Talabostat Investigator's Brochure (2006); IND No. 62,379.
22. Hollingsworth R, Leow C.C., Zhao W., Holovycky N., Chesebrough J., Rothstein R., Wetzel L., Durham N., Rios-Doria J. Doxil Synergizes with Cancer Immunotherapies to Enhance Antitumor Responses in Syngeneic Mouse Models.
23. Structures and mechanism of dipeptidyl peptidases 8 and 9, important players in cellular homeostasis and cancer. Breyan Ross, Stephan Krapp, Martin Augustin, Reiner Kierfersauer, Marcelino Arciniega, Ruth Geiss-Friedlander, and Robert Huber

24. Liu, F.; Qi, L.; Liu, B.; Liu, J.; Zhang, H.; Che, D.; Cao, J.; Shen, J.; Geng, J.; Bi, Y.; et al. Fibroblast activation protein overexpression and clinical implications in solid tumors: A meta-analysis. PLoS ONE 2015, 10, e0116683.